Quantitation in the Solid-State 13 C NMR Analysis of Soil and Organic Soil Fractions

ARTICLE *in* ANALYTICAL CHEMISTRY · JUNE 2003

Impact Factor: 5.64 · DOI: 10.1021/ac020679k · Source: PubMed

2 AUTHORS, INCLUDING:

Camille Keeler

22 PUBLICATIONS **366** CITATIONS

SEE PROFILE

Quantitation in the Solid-State ^{13}C NMR Analysis of Soil and Organic Soil Fractions

Camille Keeler and Gary E. Maciel*

Department of Chemistry, Colorado State University, Fort Collins, Colorado 80523

^{13}C CP-MAS and DP-MAS spin-counting experiments have been carried out on an absolute basis for a specific whole soil and its humin, humic acid, and fulvic acid fractions, as well as a sample of the soil that was treated with 2% HF(aq). The results confirm previous conclusions that a substantial fraction of the carbon content indicated by classic elemental analysis is missed in some samples, especially whole soil and humin, by both CP-MAS and DP-MAS ^{13}C NMR methods, and that the problem is more serious for CP-MAS than for DP-MAS. This study also confirms the fact that treatment of soil organic matter with 2% HF(aq) dramatically reduces this problem but may generate some structural uncertainties associated with significant structural alterations that accompany the HF-(aq) treatment, as indicated by the ^{13}C NMR data. The relationship between the "missing carbon" problem and the concentration of paramagnetic centers, especially Fe-(III) centers, is explored in substantial detail.

The characterization of soil organic matter has been dramatically impacted by the solid-state nuclear magnetic resonance (NMR) revolution of the past quarter century.[1,2] The development of $^{1}H \rightarrow {}^{13}C$ cross-polarization[3] and magic-angle spinning,[4] and their combination (CP-MAS),[5] provided a practical means for bringing the powerful structure elucidation capabilities of NMR to bear on solid samples of humic materials.[6,7] Accordingly, scores of papers have been published on the application of CP-MAS ^{13}C NMR in the study of humic samples,[6−15] and some studies have attempted to circumvent the CP-based difficulties of quantitating the results by using ^{13}C MAS experiments in which ^{13}C spin polarization is generated *directly* via ^{13}C spin−lattice relaxation (direct polarization, DP), rather than by CP.[7;12d,h;13] In addition, some elegant studies have been reported,[8−10,12e,14] especially by Hatcher and co-workers,[8] by Wu, Zilm, and co-workers,[9a] and by Schmidt-Rohr and co-workers,[10] which provide exquisite new details on structural−dynamical features of soil organics. The literature on the use of ^{13}C NMR for characterizing soil organics is now far too voluminous to enumerate here; nevertheless, we cite some papers that are especially relevant to the work reported here or are representative of a large body of literature, or both.[6−15]

There has long been recognition of the likelihood that paramagnetic (and perhaps ferrimagnetic or ferromagnetic) components in soil organics, even after classic fractionation procedures, can lead to major line broadening in ^{13}C NMR peaks

* To whom correspondence should be addressed. E-mail: maciel@lamar.colostate.edu.

(1) Stejskal, E. O.; Memory, J. D. *High-Resolution NMR in the Solid State*; Oxford Press: New York, 1994; Chapters 3, 4.

(2) Mehring, M. *Principles of High-Resolution NMR in Solids*; Springer-Verlag: New York, 1982.

(3) Pines, A.; Gibby, M. G.; Waugh, J. A. *J. Chem. Phys.* **1972**, *56*, 1776−1777.

(4) (a) Andrew, E. R. *Philos. Trans. R. Soc. London, Ser. A* **1981**, *299*, 505−20. (b) Andrew, E. R.; Bradbury, A.; Eades, R. G. *Nature* **1958**, *182*, 1659. (c) Kessemeier, H.; Norberg, R. E. *Phys. Rev.* **1967**, *155*, 321−337.

(5) Schaefer, J. E.; Stejskal, O. *J. Am. Chem. Soc.* **1976**, *98*, 1031−1032.

(6) (a) Axelson, D. E. *Solid State Nuclear Magnetic Resonance of Fossil Fuels: An Experimental Approach*; Multiscience Publications: Montreal, Canada, 1985. (b) *Magnetic Resonance of Carbonaceous Solids*; Botto, R. E., Sanada, Y., Eds.; Advances in Chemistry Series 229; American Chemical Society: Washington, DC, 1993; pp 175−419. (c) *NMR of Humic Substances and Coal: Techniques, Problems, and Solutions*; Wershaw, R. L., Mikita, M. A., Eds.; Lewis Publishers: Chelsea, MI, 1987; p 236.

(7) Keeler, C. Quantitative Analysis of the Uncompahgre National Forest Soil and its Extracts by ^{13}C DP- and CP-MAS Solid State NMR Methods. Ph.D. Dissertation, Colorado State University, Fort Collins, CO, 2001.

(8) (a) Hatcher, P. G. *Org. Geochem.* **1987**, *11*, 31−39. (b) Knabner, K.; Hatcher, P. G. *Sci. Total Environ.* **1989**, *81/82*, 169−177. (c) Hatcher, P. G.; Schnitzer, M.; Vassallo, A. M.; Wilson, M. A. *Geochim. Cosmochim. Acta* **1989**, *53*, 125−130. (d) Koegal-Knabner, I.; De Leeuw, J. W.; Hatcher, P. G. *Sci. Total Environ.* **1992**, *117/118*, 175−185. (e) Hatcher, P. G.; Wilson, M. A. *Org. Geochem.* **1991**, *17*, 293−299. (f) Koegel-Knabner, I.; Hatcher, P. G.; Zech, W. *Soil Sci. Soc. Am. J.* **1991**, *55*, 241−247.

(9) (a) Wu, X.; Burns, S.; Zilm, K. W. *J. Magn. Reson., Ser. A* **1994**, *111*, 29−36. (b) Keeler, C.; Maciel, G. E. *J. Mol. Struct.* **2000**, *550−551*, 297−305.

(10) (a) Mao, J.-D.; Hundal, L. S.; Thompson, M. L.; Schmidt-Rohr, K. *Environ. Sci. Technol.* **2002**, *36*, 929−936. (b) Mao, J.; Xing, B.; Schmidt-Rohr, K. *Environ. Sci. Technol.* **2001**, *35*, 1928−1934. (c) Hu, W.-G.; Mao, J.-D.; Xing, B.; Schmidt-Rohr, K. *Environ. Sci. Technol.* **2000**, *34*, 530−534.

(11) (a) Ricca, G.; Severini, F. *Geoderma* **1993**, *58*, 233−244. (b) Frund, R.; Ludemann, H.-D.; Gonzalez-Vila, F. J.; Almendros, G.; del Rio, J. C.; Martin, F. *Sci. Total Environ.* **1989**, *81/82*, 187−194. (c) Lobartini, J. C.; Tan, K. H. *Soil Sci. Soc. Am. J.* **1988**, *52*, 125−130. (d) Dereppe, J.-M.; Moreaux, C.; Debyser, Y. *Org. Geochem.* **1980**, *2*, 117−124. (e) Inbar, Y.; Chen, Y.; Hadar, Y. *Soil Sci. Soc. Am. J.* **1989**, *53*, 1695−1701. (f) Piccolo, A.; Conte, P. Advances in Nuclear Magnetic Resonance and Infrared Spectroscopies of Soil Organic Particles. In *Structure and Surface Reactions of Soil Particles*; Huang, P. M., Senesi, N., Buffle, J., Eds.; John Wiley and Sons Ltd.: New York, 1998; pp 183−250. (g) Hatcher, P. G.; Breger, I. A.; Dennis, L. W.; Maciel, G. E. ^{13}C NMR of sedimentary humic substance: New revelations on their chemical composition. In *Terrestrial and Aquatic Humic Materials*; Christman, R. F., Gjessind, O., Eds.; Ann Arbor Science Press: Ann Arbor, MI, 1983; p 37. (h) Hatcher, P. G.; Maciel, G. E.; Dennis, L. W. *Org. Geochem.* **1981**, *3*, 43−48. (i) Hatcher, P. G.; Breger, I. A.; Maciel, G. E.; Szeverenyi, N. M. In *Humic Substances in Soil, Sediment and Water: Geochemistry, Isolation and Characterization*; McKnight, D. M., Ed.; John Wiley & Sons: New York, 1985; p 275. (j) Hatcher, P. G.; Breger, I. A.; Dennis, L. W.; Maciel, G. E. Solid-state ^{13}C NMR of Sedimentary Humic Substances: New Revelations on Their Chemical Composition. In *Terrestrial and Aquatic Humic Materials*; Christman, R. F., Gjessing, O., Eds.; Ann Arbor Science Press: Ann Arbor, MI, 1983; p 47. (k) Preston, C. M.; Schnitzer, M.; Ripmeester, J. A. *Soil Soc. Am. J.* **1989**, *53*, 1442−1447. (l) Skjemstad, J. O.; Frost, R. L.; Barron, P. J. *Aust. J. Soil Res.* **1983**, *21*, 539−547. (m) Mao, J.; Hu, W.; Schmidt-Rohr, K.; Davies, G.; Ghabbour, E. A.; Xing, B. *R. Soc. Chem., G. Br.* **1999**, *228*, 79−90. (n) Watanabe, A.; Tsutsuki, K.; Kuwatsuka, S.; Kuwatsuka, K. *Sci. Total Environ.* **1989**, *81−82*, 195−200. (o) Guggenberger, G.; Zech, W.; Haumaier, L.; Christensen, B. T. *Eur. J. Soil Sci.* **1995**, *46*, 147−158.

10.1021/ac020679k CCC: $25.00
Published on Web 00/00/0000

of humic materials,[12h,13a,b,15] rendering some resonances unobservable by conventional techniques. Estimates for the loss of ^{13}C signals in ^{13}C MAS experiments, with or without CP, have ranged from ~70 to ~10%. There have also been some efforts, including very careful and detailed studies, that have focused on this quantitation problem[12d,g,h,,13−16] and in some cases on whether DP-MAS or CP-MAS techniques are more prone to these difficulties. The published body of work on this subject seems to point to Fe(III) species as the main paramagnetic culprit that causes ^{13}C signal loss in soil organics.[13−15] Some efforts have been directed at finding suitable procedures for removing Fe(III) species from soil organics, as well as other complex naturally occurring organic solids, and it appears that the best method reported to date is based on treatment with a 2% HF(aq) solution.[13c,15a]

The present paper reports a comprehensive study, including not only relative but also absolute spin-counting, on these important quantitation issues for the whole soil, humic acid, fulvic acid, and humin samples isolated from a specific site in the Uncompahgre National Forest of southwestern Colorado.[7] This paper is, as far as we know, the first report of a systematic ^{13}C spin-counting study by both CP-MAS and DP-MAS approaches on a complete suite of the classic humic fractions from the same soil—the whole soil, the humin, the humic acid, and the fulvic acid.

EXPERIMENTAL SECTION

Samples and Materials. Samples were derived from a soil with high organic content and low iron content, taken from the Uncompahgre National Forest of southern Colorado. The separation of organic fractions was, after an initial physical (sieve) removal of stones and leaf litter, based on the classic acid−base fractionation properties of humic materials,[17] as well as ion-exchange treatment (details presented elsewhere).[7] Ion exchange was carried out on a portion (A) of fulvic acid that resulted from acidification of a base extract of soil and subsequent removal of humic acid by filtration, using 20−50-mesh ion-exchange resin beads (Biorad AG 50W-8X, proton form), followed by rotary evaporation of the supernatant solution (and washings) to dryness. Another portion (B) of the acidic fulvic acid solution was dried under rotary evaporation, followed by treatment with a dry $N_2(g)$ stream. Poly(sodium 4-styrenesulfonate) and all of the intensity standards used for intensity calibrations (vide infra) were obtained from Aldrich.

Hydrofluoric Acid De-Ashing. A typical HF(aq) treatment[15a] was as follows: 4 g of soil was mixed with five aliquots (80 mL each) of 2% HF(aq) solution, stirred for 3 h and centrifuged, mixed with two 80-mL aliquots, stirred for 24 h and centrifuged, and finally mixed with one 80-mL aliquot and allowed to stir for 48 h. The supernatant solution was collected after each centrifugation step, and the final de-ashed soil was rinsed three times with distilled water and dried in air at 60 °C.

Spin-Counting Intensity References. The silicone rubber was Dow Corning 732 multipurpose sealant (poly(dimethylsiloxane) "silicone" rubber), spread onto a piece of glass and allowed to cure under room conditions for more than two months. The silicone rubber was then peeled carefully from the glass and cut into small blocks (1−2-mm edge). Typically, a weighed (70−90 mg) portion of material was packed tightly at the bottom of a 2.92-cm-long thin-walled glass tube (3-mm o.d.), which was sealed with a torch and placed in the center of the spinner with Kel-F mounts (Supporting Information Figure SI-1). A previously prepared and purified [3.2.1]bicyclo-4-pyrrolidino-*N*-methyloctan-8-one triflate compound, ^{13}C labeled at the carbonyl position (3 or 20 mg),[18] was packed into a melting point capillary tube (roughly 1.8-mm o.d. and 3.0 cm in length) and placed in the center of the spinner with Kel-F mounts and a hole drilled in the rotor cap (as shown in Figure SI-1).

EPR Experiments. EPR measurements were made in the X band at room temperature using a Bruker EMX-200 spectrometer with dual cavities, with a microwave power of 0.2 mW. The concentrations and Lande *g* values of the detected free radicals were calculated by comparison with a sample of 2,2-diphenylpicrylhydrazyl, the *g* value of which was taken as 2.0036.

Elemental Analysis. Elemental analyses were provided on finely ground (<50-μm-diameter) particles by Huffman Laboratories (Golden, CO). Total carbon content was determined by combustion under flowing oxygen at 1000 °C, followed by the coulometric detection of CO_2 on a custom-built analyzer. Total iron was determined by digestion in a mixture of nitric, hydrochloric, and perchloric acids, followed by quantification with ICP atomic emission spectroscopy. Ash contents were determined by the Water, Soil and Plant Testing Laboratory at Colorado State University by burning at 550 °C in a furnace, followed by the gravimetric determination of ash. Elemental analysis results are summarized in Table 1.

(12) (a) Preston, C. M.; Shipitalo, S.-E.; Dudley, R. L.; Fyfe, C. A.; Mathur, S. P.; Levesque, M. *Can. J. Soil Sci.* **1987**, *67*, 187−198. (b) Preston, C. M.; Ripmeester, J. A. *Can. J. Spectrosc.* **1982**, *27*, 99−105. (c) Schnitzer, M.; Preston, C. M. *Plant Soil* **1983**, *75*, 201−211. (d) Preston, C. M.; Schnitzer, M. *Soil Sci. Soc. Am. J.* **1984**, *48*, 305−311. (e) Preston, C. M. *Sci. Total Environ.* **1992**, *114*, 107−120. (f) Smernik, R.; Oades, J. M. *Solid State Nucl. Magn. Reson.* **2001**, *20*, 74−84. (g) Saiz-Jimenez, C.; Hawkins, B. L.; Maciel, G. E. *Org. Geochem.* **1986**, *9*, 277−284. (h) Mao, J.-D.; Hu, W.-G.; Schmidt-Rohr, K.; Davies, G.; Ghabbour, E. A.; Xing, B. *Soil Sci. Soc. Am. J.* **2000**, *64*, 873−884. (i) Thorn, K. A.; Steelink, C.; Wershaw, R. L. *Org. Geochem.* **1987**, *11*, 123−137. (j) Conte, P.; Piccolo, A.; van Lagen, B.; Buurman, P.; Hemminga, M. A. *Solid State Nucl. Magn. Reson.* **2002**, 158−170. (k) Frund, R.; Ludemann, H.-D. *Sci. Total Environ.* **1989**, *81/82*, 157−168. (l) Conte, P.; Piccolo, A.; van Lagen, B.; Buurman, P.; de Jager, P. A. *Geoderma* **1997**, *80*, 339−352.

(13) (a) Smernik, R. J.; Oades, J. M. *Geoderma* **2000**, *96*, 101−129. (b) Smernik, R. J.; Oades, J. M. *Geoderma* **2000**, *96*, 159−171. (c) Dai, K. H.; Johnson, C. E. *Geoderma* **1999**, *93*, 289−310.

(14) (a) Jokic, A.; Srejic, R.; Pfendt; P. A.; Zakrzewska, J. *Water, Air Soil Pollut.* **1995**, *84*, 159−173. (b) Hu, J. E.; Solun, M. S.; Taylor, G. M. V.; Pugmire, R. J.; Grant, D. M. *Energy Fuels* **2001**, *15*, 14−22.

(15) (a) Skjemstad, J. O.; Clarke, P.; Taylor, J. A.; Oades, J. M.; Newman, R. H. *Aust. J. Soil Res.* **1994**, *32*, 1215−1229. (b) Pfeffer, P. E.; Gerasimowicz, W. V.; Piotrowski, E. G. *Anal. Chem.* **1984**, *56*, 734−741. (c) Vassallo, A. M.; Wilson, M. A.; Collin, P. J.; Oades, J. M.; Waters, A. G.; Malcolm, R. L. *Anal. Chem.* **1987**, *59*, 558−562. (d) Arshad, M. A.; Ripmeester, J. A.; Schnitzer, M. *Can. J. Soil Sci.* **1988**, *68*, 593−602. (e) Schmidt, M. W.; Knicker, H.; Hatcher, P. G.; Kögel-Knabner, I. *Eur. J. Soil Sci.* **1997**, *48*, 319−328.

(16) (a) Snape, C. E.; Axelson, D. E.; Botto, R. E.; Delpuech, J. J.; Tekely, P.; Gerstein, B. C.; Pruski, M.; Maciel, G. E.; Wilson, M. A. *Fuel* **1989**, *68*, 547−560. (b) Packer, K. J.; Harris, R. K.; Kenwright, A. M.; Snape, C. E. *Fuel* **1983**, *62*, 999−1002. (c) Muntean, J. V.; Stock, L. M.; Botto, R. E. *Energy Fuels* **1988**, *2*, 108−110. (d) Dudley, R. L.; Fyfe, C. A. *Fuel* **1982**, *61*, 651−657. (e) Botto, R. E.; Wilson, R.; Winans, R. E. *Energy Fuels* **1987**, *1*, 173−181.

(17) Schnitzer, M. Organic matter characterization. In *Methods of Soil Analysis, Part 2. Chemical and Microbiological Properties*, 2nd ed.; Page, A. L.. Ed.; Agronomy Series 9 (part 2); American Society of Agronomy and Soil Science Society of America: Madison, WI, 1982; pp 581−594.

(18) Hall, R. A.; Jurkiewicz, A.; Maciel, G. E. *Anal. Chem.* **1993**, *65*, 534−538.

Table 1. Elemental Analysis and Ash Content Summary

soil component	wt of fraction (g)	% carbon from elemental analysis	% ash	% carbon on ash-free basis	% Fe from elemental analysis	total in fraction from elemental analysis (g)		% from elemental analysis			
						Fe	carbon	hydrogen	oxygen	nitrogen	sulfur
whole soil	140.43	14.81	70.30	54.12	1.05	1.47	22.51	1.92	14.71	0.89	0.10
HF-treated soil	2.15	24.36	43.60	52.88	0.25	0.0054	0.642	3.20	25.76	1.81	0.33
humin	122.77	11.86	76.80	51.12	1.07	1.31	14.56	1.51	11.96	0.62	0.07
humic acid	12.52	43.91	5.80	52.15	0.90	0.11	5.50	4.46	33.98	3.25	0.39
fulvic acid A[a] (ion-exchange treated)	7.93	21.84	47.40	41.52	0.14	0.011	3.34	2.61	22.80	1.43	0.50
fulvic acid B[b]	9.84	16.41	56.30	37.55	0.21	0.020		2.34	20.60	1.28	0.27

[a] Fraction of fulvic acid that was treated with Bio-Rad AG 50W-8X (proton-form) cation-exchange resin beads. [b] Raw fulvic acid fraction, not treated with ion-exchange resin beads.

NMR Experiments. ^{13}C NMR experiments were carried out at 25.27 MHz on a spectrometer based on a Nalorac wide-bore superconducting magnet and a home-built, two-channel console, using a Chemagnetics Phoenix data station (based on a Sun Microsystems Sparc 5), pulse programmer and receiver, home-built power amplifiers routinely capable of 300 W, and a probe with an eight-turn coil for 14-mm (o.d.) MAS rotors, with rf field strengths in both channels of 50 kHz or greater. All data acquisitions, data processing, and peak deconvolutions were performed with Chemagnetics Spinsight, Version 3.5.2.

Background signals due to the probe were obtained by simply rerunning each experiment without the corresponding sample loaded (but with the spin-counting reference in place) in the spinner under the exact same conditions as for the spin-counting experiments. The resulting background signals were deconvoluted and resynthesized using the Spinsight software to create a noise-free version of the background signal. The noise-free background signal was digitally subtracted from the spectrum of interest (i.e., of an organic soil material) to create a background-free spectrum. Background corrections were not necessary for every experiment, because, for some of the MAS NMR conditions/configurations employed, no significant background signal was generated.

RESULTS

Choice of ^{13}C NMR Configuration. The main parameters that come into play in considering the spectrometer configuration to be used for ^{13}C MAS experiments on soil organics are (1) static magnetic field strength (B_0) and (2) MAS rotor size. These and related issues have been discussed previously for the related case of coal[16a] and are mentioned here only briefly to provide perspective. It is well known that there is no resolution advantage at higher magnetic field (B_0) for ^{13}C MAS experiments on complex, amorphous organic solids. Although, other things being equal, one would usually carry out NMR experiments at the largest B_0 available, this is usually not the best choice for ^{13}C MAS experiments on soil organics, especially if one is striving for quantitation. In units of hertz, the chemical shift anisotropy (CSA) of each specific resonance is directly proportional to B_0. To avoid serious spinning sideband problems in a MAS experiment, which could render quantitation all but impossible to achieve, one must either use a sufficiently large MAS speed (roughly, greater than or equal to the CSA in Hz) or employ a sideband suppression technique, which is likely to introduce its own sources of intensity distortions. Increasing the MAS speed in parallel with choosing a high B_0 value has always been accomplished by employing MAS system designs with smaller rotor size and sample volume. Hence, the sensitivity enhancement (per gram) anticipated by using a larger B_0 is typically canceled, at least partially, by a parallel decrease in sample size. In some cases, especially if sophisticated (e.g., multiple-pulse) techniques are used, the requirements (e.g., rf homogeneity, power, or both) of the techniques may preclude the use of large samples; in such cases, since small samples are required anyhow, one might as well take advantage of the high-field sensitivity advantage (per gram).

For the ^{13}C NMR experiments reported here (CP-MAS and DP-MAS), which are rather simple and unsophisticated, we have found that a reasonable compromise configuration is a magnetic field strength of about 2.3−2.5 T (25.1−27.3 MHz for ^{13}C) and MAS rotor sizes of 14−9 mm (o.d.). Our specific configuration (2.3 T; 14-mm rotor) permits MAS speeds of 4.4−4.6 kHz, for which MAS sidebands of sp^2 carbon resonances are sufficiently small that intensity corrections are not difficult.

DP-MAS and CP-MAS ^{13}C NMR Approaches. By far the most common experimental approach for obtaining ^{13}C MAS spectra of complex organic solids (e.g., soil organics) involves the use of cross-polarization, in which ^{13}C nuclear spin magnetization is obtained via a transfer from a proton reservoir, thereby circumventing the experimental constraints of often large ^{13}C spin−lattice relaxation times (T_1) and achieving an additional signal-to-noise ratio enhancement of nominally ∼4 (the ratio of ^1H and ^{13}C magnetogyric ratios). To achieve analytical quantitation with CP-MAS ^{13}C NMR experiments, it is necessary to characterize the relevant spin dynamics parameters,[19] $T_{1\rho}^H$ (rotating-frame ^1H spin−lattice relaxation time), T_{CH} (inverse of the cross-polarization transfer rate constant), and T_1^H (^1H spin−lattice relaxation time). This time-consuming characterization is commonly not done, ostensibly in the hope that each of these parameters is individually the same across all the peaks in a given spectrum and all of the samples in a set (which, if true, would permit relative quantitation, but not absolute quantitation). In some cases, determinations of these three parameters is made for all or most of the peaks in what hopes is a sample that is representative of a set. Of course, one cannot justifiably assume that, if a given set of experimental parameters (e.g., CP contact time) is applied to all samples in a

(19) Reference 2, pp 152−154.

set, that at least relative quantitation is achieved. In the work presented here, determinations of T_1^H, $T_{1\rho}^H$, and T_{CH} were made for each relevant sample for all of the peaks with sufficient intensity to permit the determinations.

The other commonly available option for obtaining ^{13}C MAS spectra is a direct polarization (DP, no CP) approach, for which, to achieve absolute or relative quantitation, one must determine (or estimate) T_1^C values for all peaks in all (or representative?) samples sufficiently accurately so that long enough repetition delays are used (at least 4−5 times T_1^C for the largest T_1^C in a sample) or so that reliable T_1^C-based corrections can be made. Again, in the absence of reliable T_1^C information, even relative quantitation cannot be assumed just because the same repetition delay is employed for all samples in a set (and, obviously, for all peaks in a given spectrum). In the work reported here, T_1^C determinations were made on all samples for all of the peaks with sufficient intensity to generate reliable data.

Calibration of DP-MAS Intensity Reference. The carbon content of a 79.5-mg sample of silicone rubber (poly(dimethylsiloxane), PDMS) contained in the capillary (shown in Figure SI-1) was determined empirically to provide a reliable reference against which other signals could be compared in DP-MAS experiments. This was accomplished by carrying out DP-MAS measurements on weighed amounts of four reference compounds (hexamethylbenzene, glycine, L-alanine, syringic acid), each contained in separate experiments in the sample region of the rotor. To optimize or correct the results obtained in these experiments, T_1^C determinations were made on the PDMS and the four reference compounds by the Torchia method.[20] When needed, T_1^C-based corrections were made using the correction factor, C_{T_1}, given by eq 1a, which is used for situations where a

$$C_{T_1} = 1/(1 - e^{-t_d/T_1}) \quad (1a)$$

$$C_{T_1} = \frac{1}{\beta(1 - e^{-t_d/T_{1(1)}}) + (1 - \beta)(1 - e^{-t_d/T_{1(2)}})} \quad (1b)$$

single-exponential factor can describe the relaxation behavior of the peak of interest. Equation 1b is used to correct peak areas in situations where the relaxation behavior can be described satisfactorily only if two exponential factors are used. In eq 1b, β is the fraction of the relaxation component represented by $T_{1(1)}$ and $(1 - \beta)$ is the contribution from the second relaxation component, represented by $T_{1(2)}$. Mao and co-workers recently introduced a "short-cut" method for this purpose of making spin−lattice relaxation corrections.[12h]

The PDMS standard was calibrated empirically to account for a secondary quantification issue arising from spin-counting with this particular MAS configuration. The PDMS standard, located in a capillary along the rotational axis of the sample rotor, experiences a different B_1 field intensity profile than does the bulk of the sample area. Through empirical calibration, one can largely account for the effect of this location-dependent B_1 intensity on spin-counting. Results of the T_1^C determinations are collected in the Supporting Information, along with the intensity calibration results on the PDMS reference (Table SI-1). The results yield an average value of 21.8 ± 1.9 mg of natural-abundance carbon for the PDMS/capillary system (a 79.5-mg sample of pure PDMS would "ideally" contain 25.7 mg of carbon).

Calibration of CP-MAS Intensity Reference. The ^{13}C content, and ultimately the "natural-abundance equivalent", of a 6.49-mg sample of ^{13}CO-labeled [3.2.1]bicyclo-4-pyrrolidino-*N*-methyloctan-8-one triflate (compound "[3.2.1]"),[18] contained in the reference capillary (shown in Figure SI-1), was determined empirically for ^{13}C CP-MAS spin-counting measurements by carrying out the requisite CP-MAS experiments on weighed amounts of five reference compounds (hexamethylbenzene, glycine, 1,4-dimethoxybenzene, monoethyl fumarate, 2,6-dimethoxylphenol), or binary mixtures thereof, contained in the sample region of the MAS rotor. To carry out this exercise and the subsequent ^{13}C CP-MAS spin-counting of humic samples, it was necessary to determine the T_1^H, $T_{1\rho}^H$, and T_{CH} values for each relevant peak in each reference compound, and compound [3.2.1], in the relevant sample configuration (in Figure SI-1). T_1^H values were determined by the ^{13}C-detected CP-MAS/inversion−recovery method; T_1^H-based correction factors, C_{T_1} were calculated from eq 1, where $T_1 = T_1^H$ in this case.

Relative to a direct-polarization experiment, cross polarization can generate a maximum signal enhancement equal to the ratio of the γ values for the nuclei involved in the polarization transfer (in the case of ^1H-to-^{13}C cross-polarization, this ratio is 3.98). The rate of growth and decay of that enhancement during the cross-polarization period is governed by two characteristic times (inverses of the corresponding first-order rate constants), T_{CH} and $T_{1\rho}^H$. The time constant T_{CH} describes ^1H-to-^{13}C polarization transfer process leading to the growth of the ^{13}C magnetization along the ^{13}C rf field axis and $T_{1\rho}^H$ describes the decay of the spin-locked proton magnetization during CP. The maximum cross-polarization enhancement factor would be obtained with an infinitely short T_{CH} and infinitely long $T_{1\rho}^H$, yielding the theoretical maximum in intensity (M^*) for a particular CP-generated peak. Every CP-generated peak in an experimental spectrum is associated with one M^* value, which is the number that is directly proportional to the corresponding number of nuclei — i.e., the quantity we seek for quantitative analysis. The relationship between M^* and the CP-generated magnetization $M(t)$ for a specific CP period t is given in terms of the CP time constants in eq 2.[19]

$$M^* = \frac{M(t)}{\left(\frac{1}{(1 - T_{CH}/T_{1\rho}^H)}\right)(e^{-t/T_{1\rho}^H})(1 - e^{-t/T_{CH}})} \quad (2)$$

In the case where two exponential factors are needed to describe the CP process corresponding to a specific peak, eq 3 applies, where β is the fraction of component 1 and $T_{CH(1)}$, $T_{CH(2)}$,

$$M^* = \left[M(t)/\left(\left(\frac{\beta}{(1 - T_{CH(1)}/T_{1\rho(1)}^H)}\right)(e^{-t/T_{1\rho(1)}^H}) \times (1 - e^{-t/T_{CH(1)}})\right) + \left(\left(\frac{1 - \beta}{(1 - T_{CH(2)}/T_{1\rho(2)}^H)}\right)(e^{-t/T_{1\rho(2)}^H}) \times (1 - e^{-t/T_{CH(2)}})\right)\right] \quad (3)$$

(20) Torchia, D. A. *J. Magn. Reson.* **1978**, *30*, 613−616.

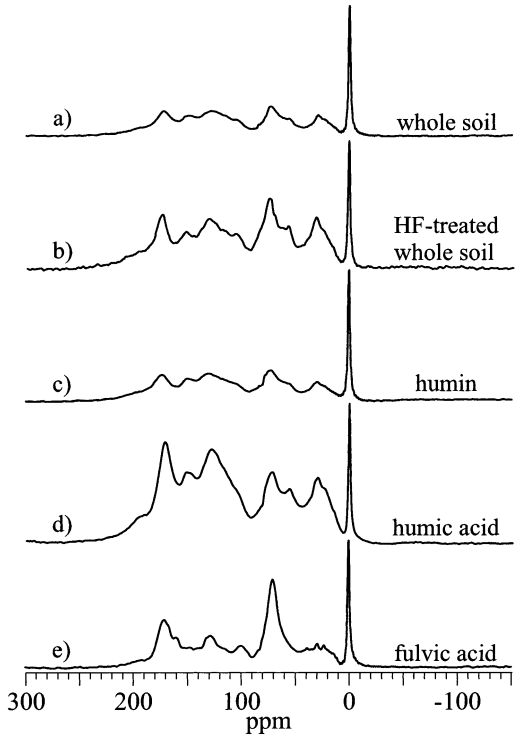

Figure 1. Carbon-13 DP-MAS spin-counting spectra of (a) Uncompahgre whole soil (1.705 g, 40 000 scans), (b) HF-treated soil (1.630 g, 10 000 scans), (c) humin (1.907 g, 40 000 scans), (d) humic acid (1.637 g, 20 000 scans), and (e) fulvic acid (1.380 g, 20 000 scans). Arbitrarily scaled for direct comparison. Silicone rubber (0 ppm) signal as intensity reference (see Figure 1).

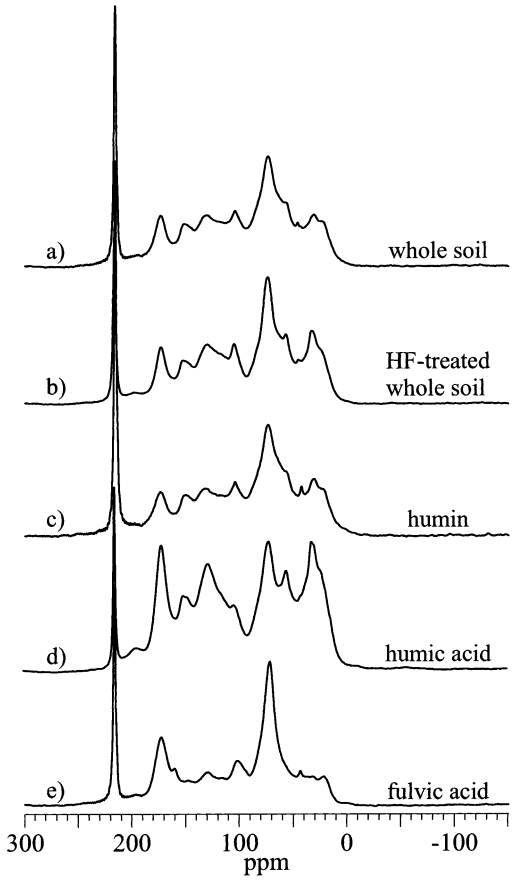

Figure 2. ^{1}H-to-^{13}C CP-MAS spin-counting spectra of the Uncompahgre whole soil and its components, arbitrarily scaled for direct comparison. In each CP-MAS experiment, 6.49 mg of the ^{13}C-labeled CP-MAS spin reference compound [3.2.1]bicyclo-4-pyrrolidino-*N*-methyloctan-8-one triflate was added as illustrated in Figure SI-1: (a) whole soil (2.237 g), (b) HF-treated soil (1.178 g), (c) humin (2.198 g), (d) humic acid (1.841 g), and (e) fulvic acid (1.483 g). Equal number of scans (80 000) for each spectrum.

$T_{1\rho(1)}$, and $T_{1\rho(2)}$ are the relevant time constants for the two components. The correction factors (C_{CP}) that correspond to eqs 2 and 3 can be obtained from those two equations by dividing both sides by $M(t)$. The relevant T_1^H results and corresponding C_{T_1} corrections (eq 1) are collected in the Supporting Information (Table SI-2), along with $T_{1\rho}^H$ and T_{CH} results obtained from variable contact time experiments (in which the CP contact time is varied systematically); the results were analyzed in terms of eq 2 or eq 3 and the corresponding C_{CP} corrections (also from eq 2 and eq 3). Also given in Table SI-2 for each peak or each reference compound is the corresponding "natural-abundance equivalent" number of milligrams of carbon corresponding to the carbonyl peak of the ^{13}CO-labeled [3.2.1] compound sealed in a capillary at the center of the rotor (Figure SI-1). The average result obtained from the empirical determinations based on the various peaks in the ^{13}C spectra of the reference compounds, or their mixtures, is 22.23 ± 1.56 mg of natural-abundance carbon (which, for a 6.49-mg sample of the [3.2.1] compound, would correspond to a ^{13}C isotopic abundance level in the carbonyl position of 93.6 ± 6.6%).

Uncompahgre Soil and Soil Components. The Uncompahgre National Forest soil (southern Colorado) was fractionated according to the procedures specified in the Experimental Section and, in more detail, elsewhere.[7] Representative ^{13}C DP-MAS and CP-MAS NMR spectra of the whole soil and its separated fractions are given in Figures 1 and 2, respectively. The tall, sharp peak at 0 ppm in Figure 1 is due to the PDMS (silicone rubber) intensity reference and the tall, sharp peak at 217 ppm in Figure 2 is due to the ^{13}CO-labeled [3.2.1] intensity reference.

Details of the chemical structure that can be extracted from spectra of the type given in Figures 1 and 2 have been the subject of numerous papers, especially noteworthy being those of Hatcher and co-workers,[8;11h,i] Schmidt-Rohr and co-workers[10] and Preston and co-workers.[11k,12a−e] Based on that literature, the huge literature that is relevant from liquid sample NMR and the study that we published on ^{13}C CP-MAS spectral editing experiments on Uncompahgre humics,[9b] we can make the "tentative" assignments shown with a representative humic acid spectrum in Figure 3. Detailed discussion and delineation of such structural assignments are presented elsewhere.[7,21]

DP-MAS ^{13}C NMR Spin Counting. Figure 1 shows each DP-MAS ^{13}C spin-counting spectrum, on a relative intensity scale, for the soil and each of the soil components. The spectra of Figure 1 were deconvoluted into contributions from specific regions of the spectra. Details of deconvolutions are available in ref 7. An example is shown for the HF-treated whole soil in Figure 4. The ^{13}C T_1 relaxation times for all the deconvoluted peaks of each of the spin-counting spectra and of the silicone rubber were derived from analogous deconvolutions of the T_1 determination spectra (ref 7) and are summarized in Tables 2 and SI-3−5, along with

(21) Keeler, C.; Kelly, E.; Maciel, G. E., manuscript in preparation.

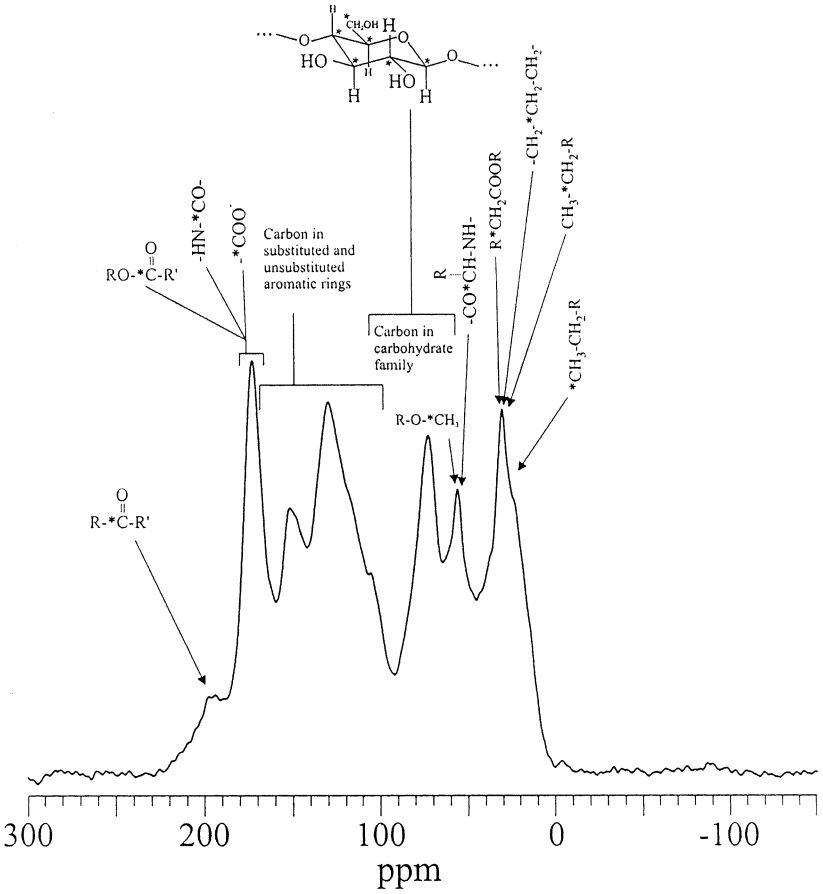

Figure 3. Typical ^{13}C CP-MAS spectrum of humic acid extracted from the Uncompahgre National Forest soil. Tentative chemical shift assignments for this humic acid are shown with arrows pointing to the peak corresponding to its representative major organic component and/or functional group.

the "T_1-corrected" peak areas (A_{corr}^{DP}) for each peak generated in the deconvolutions of the spectra of Figure 1. The corresponding amount of carbon for each peak, reported in milligrams of carbon, out of the total sample weight and as a percentage of the total carbon detected by DP-MAS spin-counting, are given in the last two columns , respectively, in Tables 2 and SI-3−5.

In Table 2 is the sum of the corresponding peak integrals in columns 4 and 5, labeled "A_{exp}^{DP}" and "A_{corr}^{DP}", not including the peak integral from the external reference. These values represent the total integral of the corresponding ^{13}C DP-MAS spin-counting spectrum and that of the T_1-corrected spectrum, respectively. The bottom of column 6 gives the total number of milligrams of carbon detected in this experiment. The error associated with each total integral was determined from the propagated error of the sum of the corresponding individual deconvoluted peaks.

The bottom of column 7 gives the calculated percent carbon in the sample based on the total T_1-corrected ^{13}C DP-MAS spin-counting integral relative to the external reference peak area. An estimated relative error for this value is reported in in parentheses, estimated by propagating the error associated with the deconvolution of the reference peak at 0 ppm, the error associated with the total T_1-corrected ^{13}C DP-MAS spin-counting integral, and that from the empirical calibration of the external reference (8.70%).

Table 3 summarizes the elemental, gravimetric, and DP-MAS spin-counting data for each soil and soil fraction. The percent carbon detected by DP-MAS spin-counting is presented along with the percent carbon detected by elemental analysis. The ratio of the percent carbon detected by DP-MAS to that detected by elemental analysis is provided in column 5. One sees that, for the whole soil and the humin, humic acid, and fulvic acid fractions of this soil, DP-MAS ^{13}C NMR detects 59−72% of the carbon measured by classic elemental analysis.

The spectra of Figure 5 are computer-generated, much like the synthetic spectra employed in the deconvolutions (e.g., Figure 4b), but have been adjusted to reflect the T_1^C-corrected peak areas (A_{corr}^{DP}) of Tables 2 and SI-3−5. Each computer-generated spectrum was created by applying the appropriate T_1 correction term (C_{T_1}) to each of the deconvoluted peaks for each spectrum. The humin (Figure 5c), humic acid (Figure 5d), and fulvic acid (Figure 5e) spectra were added, in ratios to represent their weighted contribution to the whole soil and their sample weight (Table 1), to generate a synthetic whole-soil spectrum (Figure 5f). Figure 5f (solid line) shows the experimentally obtained DP-MAS ^{13}C spectrum, C_{T_1}-weighted, of the whole soil. The overlaid spectrum, plotted with a dotted line, in Figure 5f is the whole-soil spectrum of Figure 5a. The pair of plots in Figure 5f illustrates the difference between the T_1-corrected whole-soil spectrum and the synthetic whole-soil spectrum generated by adding the appropriate ratios of the humin, humic acid, and fulvic acid spectra. The largest discrepancy between the synthetic component-generated whole-soil spectrum and the T_1-corrected whole-soil spectrum occurs in the 160−190 ppm region, where the synthetic spectrum shows significantly greater intensity.

Table 2. ^{13}C T_1 and DP-MAS Spin-Counting Results for Humic Acid (1.637 g)

ppm	carbon-13 T_1 (s)[a]	C_{T_1}[b] (±SEE %)	A_{exp}^{DP}[c] (±ERE %)	A_{corr}^{DP}[d] (±total % error)	mg of carbon[e]	% of total[f] (p_i)
197	0.207 (100)	1.00(±3.48)	77.50(±33.00)	77.50(±33.18)	14.90	2.91
172	0.07 (42.6), 0.63 (57.4)	1.00(±1.37)	452.71(±6.39)	453.16(±6.53)	87.15	17.02
150	0.102 (52.1), 0.774 (47.9)	1.00(±3.08)	299.06(±10.81)	299.88(±11.24)	57.67	11.26
130	0.068 (43), 0.607 (57)	1.00(±1.20)	544.29(±15.76)	544.72(±15.81)	104.75	20.46
115	0.121 (54.7), 0.914 (45.3)	1.01(±2.26)	192.57(±22.17)	193.68(±22.28)	37.24	7.27
104	0.044 (37.6), 0.448 (62.4)	1.00(±3.26)	131.69(±29.73)	131.70(±29.91)	25.33	4.95
72	0.092 (46.1), 0.896 (53.9)	1.01(±2.5)	349.22(±6.05)	351.41(±6.55)	67.57	13.20
56	0.056 (39.9), 0.45 (60.1)	1.00(±1.27)	193.28(±12.06)	193.29(±12.13)	37.17	7.26
39	0.044 (27.8), 0.801 (72.2)	1.00(±2.29)	69.23(±23.95)	69.57(±24.06)	13.38	2.61
30	0.115 (60.5), 1.012 (39.5)	1.01(±2.29)	199.89(±17.97)	201.42(±18.12)	38.73	7.56
20	0.08 (58.1), 0.545 (41.9)	1.00(±4.02)	146.51(±20.19)	146.55(±20.58)	28.19	5.50
0[h]	2.703 (100)	1.29(±0.47)	103.43(±4.87)	133.92(±4.89)	25.75(±8.70)[g]	
	total (not including reference at 0 ppm)		2655.96(±4.86)[i]	2662.88(±4.91)[i]	512.03	100%
	total % carbon by DP-MAS spin-counting				31.3(±11.1)[j]	

[a] Parameters are from computer output and, in some cases, carry more digits than are statistically significant. ^{13}C T_1's reported as single- or multiple-component values with the percentage contribution from each relaxation component reported in parentheses. [b] ^{13}C T_1 correction term as shown in eq 1, with error estimated from the standard error of the estimate (SEE). [c] The experimental peak areas with the estimated relative error (ERE) given in parentheses (based on 20 independent deconvolutions). [d] Raw peak areas for each deconvoluted peak multiplied by the relaxation correction factor (C_{T_1}). The total relative error is given as a percent error in parentheses and is propagated from the error of the ^{13}C T_1 correction term and that of the experimental peak area. [e] Amount of carbon in milligrams per deconvoluted peak in the whole spinner sample (1.637 g). [f] Percent carbon of the DP-MAS detected carbon, $p_i = 100$(mg of C for peak i)/(sum of mg of C for all peaks). [g] Result and percent relative error from calibration of capillary containing 79.5 mg of silicone rubber with standard materials. [h] Peak due to silicone rubber external reference. [i] Sum of the individual peak integrals in the same column, excluding the integral due to the reference material at 0 ppm. The error for this total is the propagated error of the sum of the aforementioned integrals. [j] The total percent carbon with relative error given in parentheses. Error for this total is the propagated error of the total corrected peak integral, and the errors associated with the external reference. [k] All numbers in parentheses are percents.

Table 3. Summary of Results from ^{13}C DP-MAS Spin-Counting

soil component	wt % of soil	% C by DP-MAS spin-counting	% C by elem anal.	(amt of C detected by DP-MAS)/(amt of C detected by elem anal.) × 100%
whole soil	100	9.5	16.07	59.1
HF-treated soil	n/a	25.6	29.88	85.7
humin	87.42	8.5	11.86	71.7
humic acid	8.92	31.3	43.91	71.3
fulvic acid[a]	3.66	15.0	21.84	68.7

[a] Elemental and DP-MAS data are that of the ion-exchange-treated fulvic acid.

Error associated with the ^{13}C T_1 determinations was propagated to the correction factor (C_{DP}) and presented as a relative deviation in Table 2. This error was calculated from the standard error of the estimate (SEE) in each ^{13}C T_1 regression analysis and was determined using the SigmaPlot 5.0 program. The relative standard deviation associated with each deconvoluted peak area of each of the ^{13}C DP-MAS spin-counting experiments was estimated by finding the relative standard deviation for each peak of interest in 20 nonsequential deconvolutions of each of the DP-MAS spin-counting spectra shown in Figure 1 (and Figure 4). These values are reported in column 4 of Table 2. This estimated error reflects the large uncertainty in peak areas typically encountered when broad, superimposed peaks are deconvoluted.

The total of the peak integrals (A_{exp}^{DP}), before being multiplied by the correction term (C_{T_1}), is shown at the bottom of column 4 in Table 2 (and in Tables SI-3−5). The error for this total, and for that of the T_1^C-corrected peak areas (A_{corr}^{DP}), is propagated from the sum of the values printed in that particular column. The error associated with the number of milligrams of carbon for the reference material peak at 0 ppm is that from the relative standard deviation of the calibration trials (as presented in Table SI-1). The error associated with the total percent carbon was determined by propagating the error of the total corrected peak area, the error associated with calibrating the external reference, and the error of the corrected peak area for the external reference.

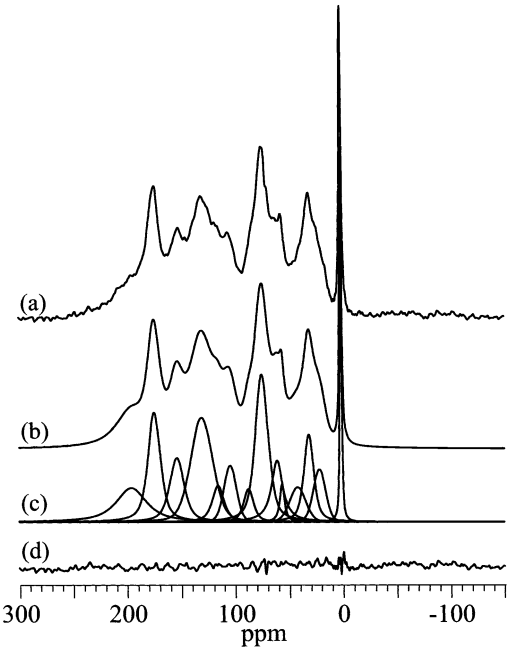

Figure 4. Carbon-13 DP-MAS spectrum of HF-treated Uncompahgre whole soil (1.630 g) and 79.5 mg of silicone rubber external reference (10 000 scans). The uppermost spectrum (a) represents the experimental spectrum. The result from the deconvolution of spectrum a is shown in (c) as individual peaks. The "synthetic" spectrum b is the sum of the peaks of (c). Spectrum d is the difference of spectrum a minus spectrum b.

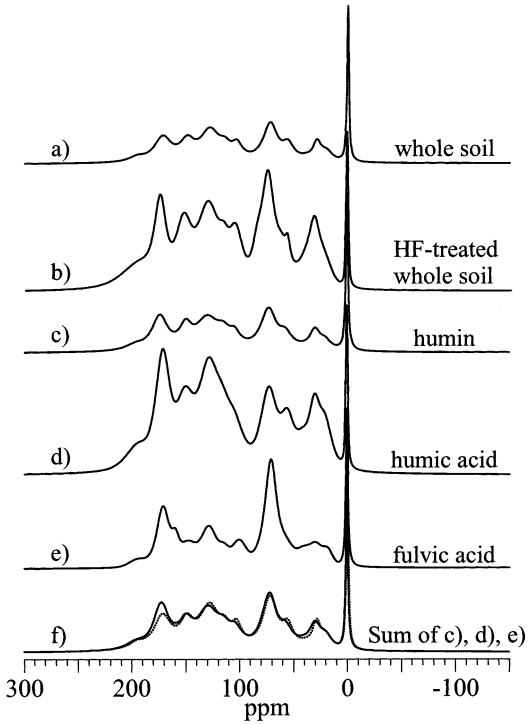

Figure 5. Computer-generated "T_1-corrected" spectra of (a) 1.705 g of whole soil, (b) 1.630 g of HF-treated soil, (c) 1.907 g of humin fraction, (d) 1.637 g of humic acid, and (e) 1.380 g of fulvic acid. Spectra a−e were created by taking the synthetic spectra generated by deconvolution of the spectra of Figure 2 and applying the appropriate T_1 correction factors (C_{T_1}) to each deconvoluted peak needed to generate the total synthetic spectrum. Spectrum f is a computer-generated whole-soil spectrum, created by summing the humin, humic, and fulvic spectra with amplitude corrections as demonstrated in the following relationship: ((0.782 × spectrum c) + (0.0929 × spectrum d) + (0.157 × spectrum e)). These amplitude corrections were made to reflect the actual amount of each fraction extracted from the whole soil and to correct for the different sample sizes. Spectrum f also shows the spectrum of the whole soil (Figure 5a) overlaid and plotted with a dotted line.

CP-MAS ^{13}C NMR Spin Counting. Figure 2 shows each CP-MAS ^{13}C spectrum, on an adjusted vertical scale, for the soil and each of the soil components. The spectra of Figure 2 were deconvoluted into contributions from specific regions of the spectra,[7] as in the DP-MAS example shown in Figure 4. ^{13}C-detected ^{1}H inversion−recovery CP-MAS determinations of T_1^H were carried out on all of the samples represented in Figure 3 and the ^{13}C-labeled [3.2.1] intensity reference, and it was found that T_1^H values corresponding to all peaks, except the ^{13}CO-[3.2.1] reference peak, are sufficiently short (≪300 ms) that T_1^H-based corrections are not necessary for the 1-s repetition delay employed in the spin-counting experiments. A T_1^H value of 0.78 s was determined for the ^{13}CO peak of [3.2.1], so a corresponding C_{T_1} correction of 1.384 was applied for that peak.

Variable-contact-time CP-MAS ^{13}C experiments were carried out on all the samples represented in Figure 2. T_{CH} and $T_{1\rho}^H$ values were derived from these experiments for each deconvoluted peak area (see Figure 4), and for the ^{13}CO-[3.2.1] peak, and were used in eqs 2 and 3 to calculate CP correction factors, C_{CP}, to correct the experimentally determined deconvoluted peak areas, A_{exp}^{CP}, according to eq 4, where $C_{T_1} = 1$ for all the peaks of the humic materials. Values of $T_{1\rho}^H$ and T_{CH}, as well as β for peaks that behave as two-component systems (eq 3), are collected, along with A_{corr}^{CP} values, in Tables 4 and SI-6−8 for the humic acid for the whole soil, the humin, and the fulvic acid, respectively. The corresponding amount of carbon for each peak, reported in milligrams of carbon, out of the total sample weight and as a percentage of total carbon detected by CP-MAS spin-counting, are also given respectively in columns 10 and 11 of Tables 4 and SI-6−8.

$$A_{corr}^{CP} = A_{exp}^{CP} C_{T_1} C_{CP} \quad (4)$$

The totals of columns 8 and 9 in Table 4 give the sums of the corresponding peak integrals,

The calculated percent carbon in the sample based on the total C_{CP}-corrected ^{13}C CP-MAS spin-counting integral relative to the external reference peak area is given in column 10. An estimated relative error for this value is shown in parentheses, estimated by propagating the error associated with the deconvolution of the reference peak at 217 ppm, the error associated with the total C_{CP}-corrected ^{13}C CP-MAS spin-counting integral, and that from the empirical calibration of the external reference (7.0%).

Table 5 summarizes the elemental, gravimetric, and CP-MAS spin-counting data for the soil and each soil fraction. The percent carbon detected by CP-MAS spin-counting is presented along with the percent carbon detected by elemental analysis. The percentage of carbon detected by CP-MAS relative to that detected by elemental analysis is seen in Table 5 to be 48.4% for the whole soil, 54.6% for the humin, 68.5% for the humic acid, and 65.8% for the fulvic acid.

Effects of Unpaired Electrons. One method that has been suggested previously for the removal from soil organics of ferrimagnetic or ferromagnetic and/or paramagnetic metal compounds, which are believed to be at least partly responsible for "signal loss" in NMR spectra of soils and soil fractions, is treatment with dilute HF(aq).[13,15] Accordingly, the Uncompahgre soil was treated with 2% aqueous HF, and the resulting HF-treated soil was examined in the same manner as discussed for the classical soil fractions above. DP-MAS and CP-MAS ^{13}C spin-counting spectra of the HF-treated soil are included in Figures 1 and 2. The DP-MAS and CP-MAS ^{13}C spin-counting results on this sample are collected in the Supporting Information (Tables SI-9 and SI-10); Tables 3 and 5 include this sample in the spin-counting summaries. One sees that, in keeping with expectations based on prevailing assumptions, HF treatment increases the percent carbon detected by solid-state ^{13}C NMR, from 59.1 to 85.7% for the DP-MAS case and from 48.4 to 82.0% for CP-MAS. The elemental analysis results in Table 1 show that this HF(aq) treatment reduced the Fe content of the soil from 1.05 to 0.25%.

To explore the implied hypothesis that Fe(III) content is primarily responsible for rendering a substantial portion of the carbon in humic materials "invisible" in solid-state ^{13}C NMR, additional experiments were carried out. A series of Fe(III)-containing humic acid samples was prepared by exposing the humic acid to an $Fe(NO_3)_3$(aq) solution in a stirred slurry at room temperature, followed by drying on a rotary evaporator and then at 60 °C in an oven for several hours. The ^{13}C DP-MAS spectra obtained on the $Fe(NO_3)_3$-containing solid humic samples isolated from these treatments are shown in Figure 6, which also gives the total ^{13}C NMR integrals (not counting the [3.2.1] signal) and

Table 4. ^{13}C CP-MAS Spin-Counting Results for the Humic Acid (1.842 g)[a]

	cross-polarization parameters									
	T_{CH} (ms)		$T_{1\rho}$ (ms)							
ppm	(1)	(2)	(1)	(2)	β	C_{CP}[b] (±SEE %)	A_{exp}^{CP}[c] (±ERE %)	A_{corr}^{CP}[d] (±total % error)	mg of carbon[e]	% of total[f] (p_i)
197	0.498		3.944			1.36(±4.71)	1347(±12.4)	1834.1(±13.3)	11.75	2.06
172	0.299		3.586			1.27(±1.71)	8086.9(±4.8)	10275.9(±5.1)	65.83	11.53
150	1.284	0.193	2.474	5.559	0.70	1.78(±2.05)	5574.4(±9.0)	9909.3(±9.3)	63.48	11.12
130	0.025	0.411	0.410	4.010	0.26	1.68(±2.17)	9463.4(±7.5)	15921.4(±7.8)	102.00	17.86
115	0.018	1.154	5.403	1.934	0.52	1.56(±3.80)	3965.6(±27.7)	6168.1(±27.9)	39.51	6.92
104	0.047		3.907			1.28(±6.75)	2146.7(±23.4)	2739.7(±24.3)	17.55	3.07
72	0.020	0.350	3.340	0.795	0.63	1.61(±3.49)	10807.0(±5.5)	17407.0(±6.5)	111.51	19.53
56	0.022	0.271	3.941	1.161	0.67	1.44(±3.48)	5311.8(± 8.9)	7664.4(±9.5)	49.10	8.60
39	0.020		3.110			1.37(±5.72)	4097.8(±15.9)	5615.6(±16.9)	35.97	6.30
20	0.022	0.239	2.795	6.912	0.74	1.33(±3.28)	3489.8(±26.2)	4654.4(±26.4)	29.82	5.22
10	0.029	0.184	2.336	5.332	0.58	1.35(±2.52)	5155.3(±13.8)	6960.9(±14.0)	44.59	7.81
217[g]	0.420		198.0			1.53(±1.13)	2274.6(± 1.9)	3470.6(±2.2)	22.23(±7.0)[h]	
	total (not including reference at 217 ppm)						59445.7(±3.7)[i]	89150.6(±3.8)[i]	571.12	100.00
	total % C by CP-MAS spin-counting						31.0(±8.3)[j]			

[a] All values given as the computer output, in some cases with more integers stated than are statistically significant. Cross-polarization time constants reported as single- or multiple-component values. For single-exponential component growth/decay, one constant is reported for T_{CH} and $T_{1\rho}$. For multiple-component exponential behavior, the value for each component is listed under (1) and (2), with the contribution from component 1 reported in the column titled with the β symbol. The contribution from component 2 will then be $(1 - \beta)$. [b] Calculated cross-polarization correction factors for each peak from eqs 2 and 3, with error estimated from the standard error of the estimate (SEE). [c] Experimental peak areas for each deconvoluted peak. The estimated relative error (ERE) is given as a percent error in parentheses. The estimated relative error is based on 20 independent deconvolutions. [d] Experimental peak areas multiplied by the ^1H T_1 relaxation correction factor (C_{T_1}) and cross-polarization correction factor (C_{CP}). The ^1H T_1 correction factor will be 1 for all the peaks of the soil or soil extract and 1.38 for the external reference (peak at 217 ppm). The total error is given as a percent error in parentheses. The total error is the propagated error of the correction term and experimental peak area. [e] Amount of carbon in milligrams per deconvoluted peak out of the whole spinner sample (1.842 g). [f] Percent carbon contribution from this peak out of the total CP-MAS detected carbon, $p_i = 100$(mg of C for peak i)/(sum of mg of C for all peaks). [g] Peak due to [3.2.1] bicyclo compound external reference. [h] Result from the calibration of the [3.2.1] reference compound. [i] Sum of the individual peak integrals in the same column, excluding the integral due to the reference material at 217 ppm. The error for this total is the propagated error of the sum of the aforementioned integrals. [j] The total percent carbon with relative error given in parentheses. Error for this total is the propagated error of the total corrected peak integral, and the errors associated with the external reference.

Table 5. Summary of Results from CP-MAS Spin-Counting

		% carbon		
soil component	wt % of soil	by elem anal.	by CP-MAS spin-counting	detected by CP-MAS spin-counting[a]
whole soil	100	16.07	9.0	48.4
HF-treated soil	n/a	29.88	24.5	82.0
humin	87.42	11.86	6.7	54.6
humic acid	8.92	43.91	31.0	68.5
fulvic acid	3.66	21.84	14.3	65.8

[a] Calculated by (% C by CP-MAS)/(% C by elem anal.) × 100%.

the elemental iron contents measured for these samples. One sees that, as the Fe content is increased, the observed DP-MAS ^{13}C NMR spectrum is attenuated in intensity. Analogous results are seen in Figure 7 for a series of samples prepared in a manner similar to the method used for the samples of Figure 6, except the substrate was a material of well-known structure, poly(sodium-4-styrene sulfonate), for which the largest T_1^C was measured to be approximately 16 s.

The series of samples that is represented in Figure 6 was also studied by EPR.[22] Figure 8 shows the relevant segments of the EPR spectra of that series of samples. Centered at a g value of 4.37, which has been identified as characteristic of Fe^{3+},[22c] one sees in the spectra, as expected, a monotonic increase in integrated EPR intensity (double integration of the common derivative EPR display) up to an added amount of $Fe(NO_3)_3 \cdot 9H_2O$ (initially introduced as an aqueous solution) of 962 mg/2.5 g of humic acid. At this Fe(III) loading level, the EPR intensity has doubled back for the highest two loading levels. Interestingly, the intensity of the EPR signal at $g = 2.02$, which is characteristic of organic free radicals, decreases monotonically with increasing Fe(III) loading level.

DISCUSSION

The results described above confirm in a quantitative manner the prevailing view that the application of solid-state ^{13}C MAS methods to soil organics, using either CP or DP, suffers from a loss of ^{13}C signal intensity relative to what would be expected from the carbon content determined by classic elemental analysis. The ranges of signal loss measured for the whole Uncompahgre soil and its classic fractionation components (Tables 3 and 5) are in a range that is consistent with the magnitudes reported previously. As has been reported previously for other soil organics, the magnitude of the "invisible carbon" is larger for the CP-MAS than for the DP-MAS approach.[12d,h,13,15]

The origin of the CP-versus-DP deficiency is not clear. There is no doubt that the technical demands (e.g., rf power and rf homogeneity) are greater for CP than for DP experiments,[23] so one might initially think that this could be the reason for the CP-versus-DP difference. One might make a convincing argument

(22) (a) Senesi, N. *Adv. Soil Sci.* **1990**, *20*, 77−130. (b) Senesi, N.; Sposito, G.; Martin, J. P. *Sci. Total Environ.* **1986**, *55*, 351−362. (c) Senesi, N.; Griffith, S. M.; Schnitzer, M. *Geochim. Cosmochim. Acta* **1977**, *41*, 969−976.

(23) (a) Campbell, G. C.; Galya, L. G.; Beeler, A. J.; English, A. D. *J. Magn. Reson., Ser. A* **1995**, *112*, 225−228. (b) Privalov, A. F.; Dvinskikh, S. V.; Vieth, H.-M. *J. Magn. Reson. Ser. A* **1996**, *123*, 157−160.

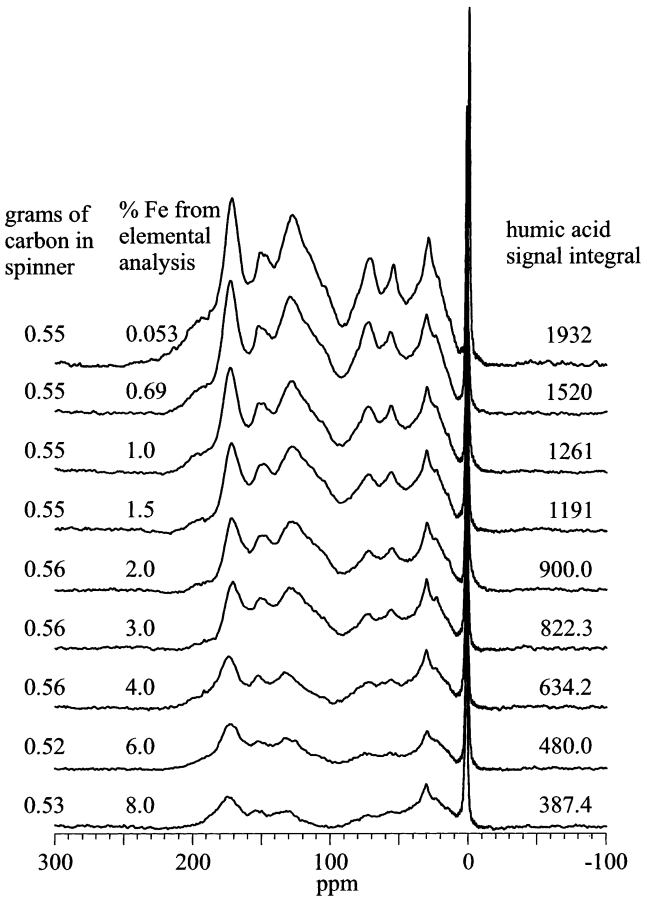

Figure 6. ^{13}C DP-MAS spin-counting spectra of the Uncompahgre humic treated with $Fe(NO_3)(aq)$, with the resulting Fe contents indicated. Equal number of scans (16 000) for all spectra; repetition delay, 4.0 s; 79.5 mg of silicone rubber external standard at 0 ppm.

for this point of view, to which we gave substantial attention,[7] had our CP-MAS and DP-MAS reference calibrations been based on simple weighing of the samples inserted into the capillaries. However, our calibrations were carried out empirically, comparing against weighed amounts of "standard compounds" placed in the same rotor space as occupied by the soil organics in the spin-counting experiments and therefore experiencing the same rf deficiencies in the calibration experiments as did the soil organics during spin-counting. Thus, rf imperfection effects should largely cancel and are not likely to be the source of the deficiency of CP-MAS relative to DP-MAS in this study. It seems more reasonable that the paramagnetic components that are likely to be largely responsible for the "invisible carbon" syndrome in both CP-MAS and DP-MAS experiments have a more deleterious effect on the former than the latter, perhaps by reducing the $T_{1\rho}^{H}$ values of some protons that "should be" important in CP to values that are so small that such protons are not effective in cross polarization.

In Figure 5f, where the "synthetic" (computer-generated) whole-soil DP-MAS spectrum is compared to the DP-MAS T_1^C-corrected whole-soil spectrum, one can see that there is a clear intensity difference for the peak centered at 172 ppm; i.e., we observe more carbon in the region at 172 ppm for the extracted components than for the whole soil. It is interesting to note that roughly 70% of the carbon was spin-counted (compared to classic elemental analysis) in each of the spectra used to generate the "synthetic" whole-soil spectrum, while we were only able to account for roughly 59% of the carbon in the DP-MAS spectrum of whole soil. This discrepancy may account for the intensity mismatch between the "synthetic" and T_1^C-corrected spectrum. Why there is a discrepancy between the percent carbon observed by NMR for the whole soil versus that of the humin sample is unclear. It is possible that some of the iron changed its location relative to carbon centers during the extraction procedure.

The results shown in Tables 3 and 5 confirm previous reports of improved ^{13}C NMR detection capability for soil organics that have been treated with 2% HF(aq). And, the fact that 2% HF(aq) treatment is also accompanied by a reduction in the amount of iron in a sample confirms previous reports on other complex, naturally occurring organic solids and lends support to the basic premise of this technique in its development by Skjemstad and co-workers.[15a] The results shown in Figures 6 −8 lend further support, albeit not cause-and-effect proof, of the relationship between Fe(III) content and the severity of the "invisible carbon" problem. This is seen in more graphical form in Figure 9, which shows, for Fe loading levels up to ∼4%, a roughly linear relationship between the percent carbon observed in DP-MAS spin-counting experiments and the percent Fe contained in a set of Uncompahgre humic acid samples prepared with varying amounts of Fe(III). This figure also shows the percent ^{13}C-observed values predicted according to a previously described theoretical model[24] in which no ^{13}C nuclei that are within a given distance (0.97 nm in the present case) of a paramagnetic center (Fe^{3+} in this case) can be observed in high-resolution ^{13}C NMR experiments. One sees moderately good agreement with this simple model up to Fe amounts of roughly 3%, much higher than what is present in the Uncompahgre soil.

The presence and manifestation of paramagnetic Fe(III) centers in humic samples is underscored by the EPR spectra shown in Figure 8 for a series of humic acid samples to which varying amounts of Fe^{3+} had been added. The monotonic increase in EPR signal intensity at $g = 4.37$ with increasing Fe(III) content for the lowest seven Fe(III) contents is expected, but the turnaround for the highest two Fe(III) contents is not. This turnaround may come about at the highest Fe(III) concentrations because (a) the added Fe(III) has reached a level at which "saturation" of chemisorption sites has occurred or (b) the paramagnetic centers are sufficiently close together to bring about electron-spin/electron-spin interactions and exchange.[25] Figure 8 also shows the somewhat unexpected result that, with the exception of the first Fe^{3+} increment, increasing the Fe(III) content of the humic acid leads to a decrease in the concentration of organic free radicals, which generate the EPR signal at $g = 2.02$. A possible explanation for this trend is that Fe^{3+} addition leads to a quenching of some free radicals, e.g., by facilitating coupling reactions or other radical annihilation processes. One also sees in Figure 8 that treatment of the humic acid with 2%

(24) Lock, H.; Wind, R. A.; Maciel, G. E.; Johnson, C. E. *J. Chem. Phys.* **1993**, *99*, 3363−3373.

(25) (a) Lewis, I. C.; Singer, L. S. Electron Spin Resonance and the Mechanism of Caronization. In *Chemistry and Physics of Carbon*; Marcel Dekker: New York, 1981; Vol. 17. (b) Pake, G. E.; Estle, T. L. *The Physical Principles of Electron Paramagnetic Resonance*, 2nd ed.; Advanced Book Program; W. A. Benjamin: Reading, MA, 1973; Chapter 6. (c) Jackson, C.; Wynne-Jones, W. F. K. *Carbon* **1964**, *2*, 227−237.

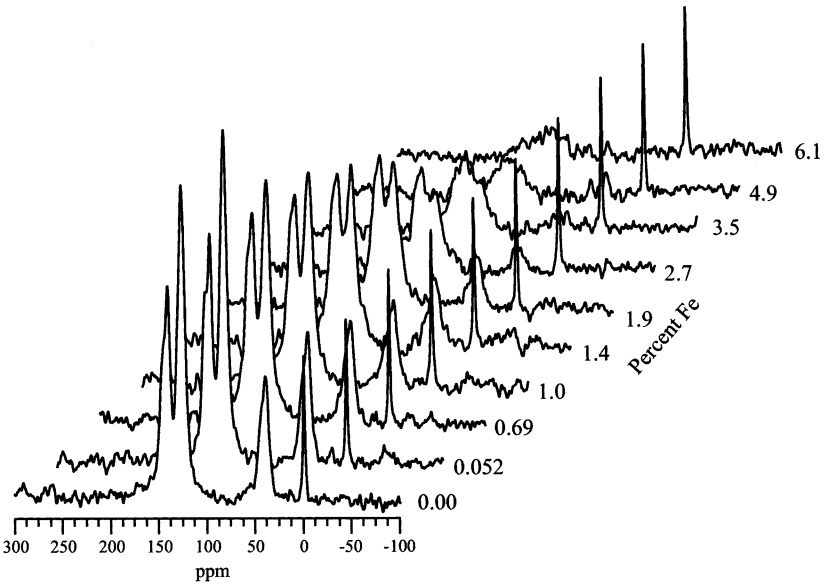

Figure 7. ^{13}C DP-MAS spin-counting spectra of poly(sodium 4-styrenesulfonate) treated with $Fe(NO_3)(aq)$, with the resulting percent Fe for each sample indicated on the figure. Equal number of scans (360) for all spectra; repetition delay, 60 s; 79.5 mg of silicone rubber external standard at 0 ppm.

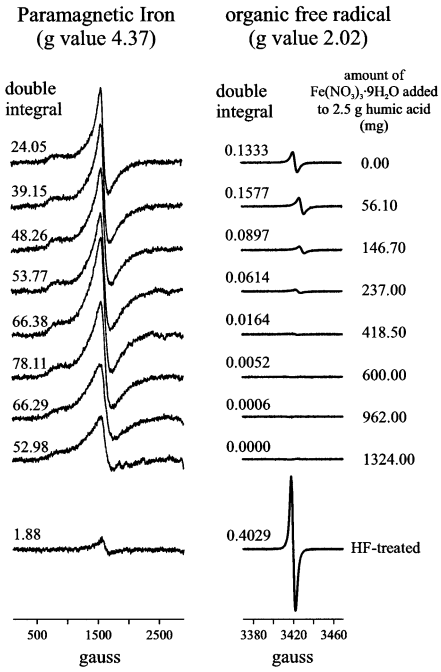

Figure 8. EPR spectra of Uncompahgre humic acid samples of Figure 6 (i.e., with variable amounts of Fe(III) added as $Fe(NO_3)_3$-(aq)), showing integrated intensities (double integrals) for the two spectral regions indicated. Bottom: EPR spectrum of humic acid sample that had been treated with 2% HF(aq). Equal number of scans (16) for each spectrum.

HF(aq) dramatically decreases the Fe(III) signal at $g = 4.37$ and dramatically increases the organic free radical signal at $g = 2.02$. The effect on the Fe(III) signal is expected, at least qualitatively, but the increase in the free radical content is not straightforward. It seems unlikely that treatment with dilute aqueous HF would generate free radicals in the usual sense, i.e., by breaking covalent bonds; this intensity increase implies that the quenching referred to above may involve Fe(III)/radical interactions that are more physical than chemical and are reversible.

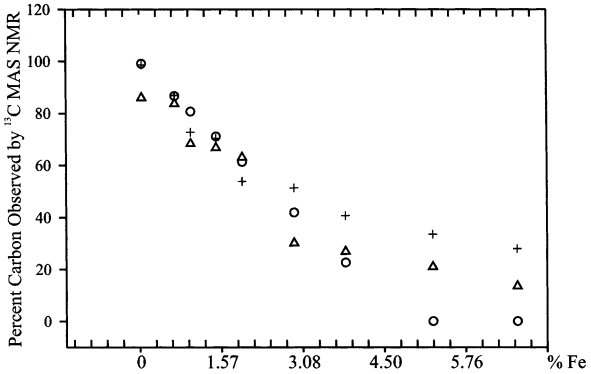

Figure 9. Percent ^{13}C observed in DP-MAS experiments as a function of the Fe(III) content obtained by treatment of the humic acid with $Fe(NO_3)_3(aq)$. Fe(III)-containing humic acid samples (+), Fe-(III)-containing poly(sodium 4-styrenesulfonate) samples (Δ), and predictions of simple theoretical model (○).

The HF treatment results of this study support the contention that this is the "best" treatment so far described in the literature for minimizing the "invisible carbon" problem. Close inspection and comparisons of information provided in the Supporting Information (Tables SI-3 and SI-9 and Tables SI-6 and SI-10) reveal significant differences, some of them substantial, between the relative concentrations of the various structural regions of the whole soil and the HF-treated soil. These differences are in most cases not dramatic, and any interpretations at this point must be considered highly speculative. The most substantial differences are seen primarily at 197 (which might reflect acid-catalyzed aldol-type condensation reactions), at 104 (which might reflect conversions of carbohydrate moieties) and at 39 ppm (which might reflect an increase in branched aliphatics, possibly caused by some type of acid-catalyzed rearrangement(s)). In any case, the experimental errors in the solid-state ^{13}C NMR data given here are sufficiently large, and the relevant peak intensities sufficiently small, to preclude any definitive conclusions regarding HF(aq)-generated structural transformations.

In summary, as attractive as the 2% HF(aq) treatment may be in comparison with other methods for reducing paramagnetic effects on the ^{13}C spectra of soil organics, this treatment may bring about, not surprisingly, some significant, albeit not dramatic, changes in organic structure. Of course, one expects some changes in the relative and absolute abundances of various regions of the ^{13}C NMR spectrum as complexed Fe(III) is removed from specific structural sites, even if there is no transformation of the organic structure. For example, one might expect an increase in integrated intensity in the region of carboxylic or phenolic carbon, or both (~155−175 ppm) as complexed Fe(III) is removed. Figure 5f appears to show that more carbon is observed in the 172 ppm region for the extracted components than for the whole soil. However, one does not see such an effect on the numerical DP-MAS intensities at 172 or at 150 ppm (in Tables SI-3 and SI-9 for the whole soil and HF-treated soil, respectively), nor does one see such a trend in the tabulated CP-MAS results (Tables SI-6 and SI-10). Thus, it appears that some organic structural transformations may accompany treatment with 2% HF(aq), but such transformations, if indeed they occur, are not well characterized or understood, as concluded earlier.[13c] This is a subject that may require further research.

ACKNOWLEDGMENT

The authors gratefully acknowledge support of this research by U.S. Department of Energy Grant DE-FG0395ER14558.

SUPPORTING INFORMATION AVAILABLE

Ten tables that summarize relevant relaxation results and details of their manifestation in deriving the spin-counting results, as well as a figure and text that describe the MAS rotor design that was employed. This material is available free of charge via the Internet at http://pubs.acs.org.

Received for review November 4, 2002. Accepted February 25, 2003.

AC020679K